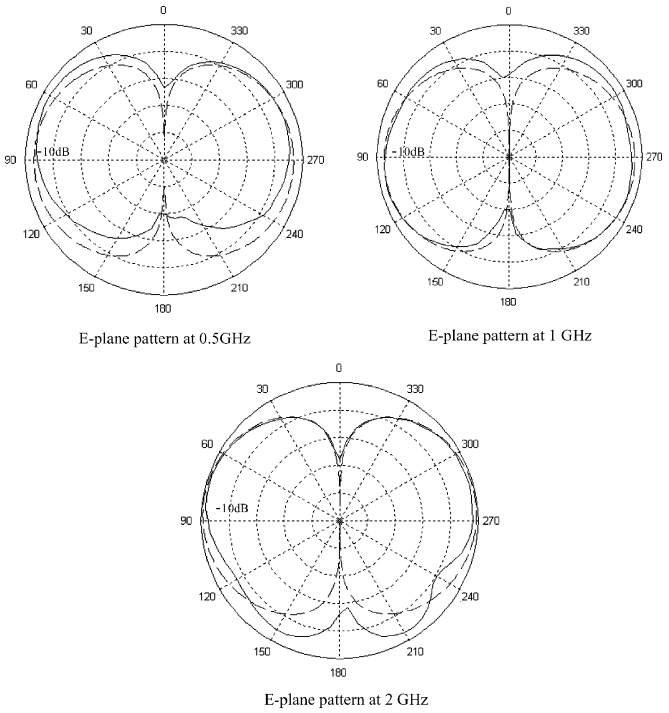

Fig. 9. Radiation patterns [measured (–) and simulated $(\cdots)$] of E_θ-component in the E-plane.

IV. Conclusion

A wide-band top loaded dual sleeve antenna, employing broad-banding techniques has been investigated numerically and experimentally and is shown to yield an impedance bandwidth ratio of 4.2:1 for a VSWR of less than 2.0:1. The typical antenna radiation pattern behavior has also been observed over the bandwidth. The symmetrical structure of the antenna offers radiation pattern stability in the operating frequency band. An attractive feature of the antenna is its compact size due to the considerably small ground plane. The antenna is proposed as a suitable option for broadband mobile and vehicular communication.

References

[1] H. Kawakami and G. Sato, "Boadband characteristics of rotationally symmetric antennas and thin wire constructs," *IEEE Trans. Antennas Propag.*, vol. AP-35, no. 1, pp. 26–32, Jan. 1987.

[2] S. D. Rogers and C. M. Butler, "Cage antennas optimized for bandwidth," *Electron. Lett.*, vol. 36, no. 11, pp. 932–933, 2000.

[3] W. Cho, M. Kanda, H. Hwang, and M. W. Howard, "A disc-loaded thick cylindrical dipole antenna for validation of a EMI test site from 30 to 300 MHz," *IEEE Trans. Electromagn. Compat.*, vol. 42, pp. 172–180, May 2000.

[4] M. J. Ammann and Z. N. Chen, "A wide-band shorted planar monopole with bevel," *IEEE Trans. Antennas Propag.*, vol. AP-51, no. 4, pp. 901–903, Apr. 2003.

[5] E. L. Bock, J. A. Nelson, and A. Dorne, "Sleeve antennas," in *Very High Frequency Techniques*. New York: McGraw Hill, 1947, ch. 5, pp. 119–137.

[6] A. J. Poggio and P. E. Mayes, "Pattern bandwidth optimization of the sleeve monopole antenna," *IEEE Trans. Antennas Propag.*, vol. AP-14, no. 5, pp. 643–645, Sep. 1966.

[7] A. D. Wunsch, "Fourier series treatment of the sleeve monopole antenna," *Proc. Inst. Elect. Eng.*, pt. H, vol. 135, no. 4, pp. 217–225, Aug. 1988.

[8] R. W. P. King and T. T. Wu, "The cylindrical antenna with arbitrary driving point," *IEEE Trans. Antennas Propag.*, vol. AP-13, pp. 710–718, Sep. 1965.

[9] T. L. Simpson, "The disc loaded monopole antenna," *IEEE Trans. Antennas Propag.*, vol. 52, no. 2, pp. 542–550, Feb. 2004.

Accelerated Computation of the Free Space Green's Function of Semi-Infinite Phased Arrays of Dipoles

Christophe Craeye and Filippo Capolino

***Abstract*—In this Communication, we provide an efficient algorithm for the evaluation of the semi-infinite array Green's function (SAGF) for a semi-infinite planar periodic phased array of dipoles in free space. For observation points not too far from the array plane, the algorithm uses a hybrid spectral-spatial representation of the Green's function accelerated with the Levin T method, that we show to be faster than the Shanks method. For observation points sufficiently far away from the array plane, we show that the SAGF is efficiently evaluated by using asymptotic field expressions. Asymptotics is also used to explain the loss of accuracy of the Levin T accelerator in certain regions, and a correction procedure is proposed to overcome this problem.**

***Index Terms*—Arrays, Green's function, numerical methods, periodic structures.**

I. Introduction

In a previous paper [1], one of the authors presented a method for the fast computation of the scalar semi-infinite array Green's function (SAGF) related to semi-infinite planar phased arrays of dipoles, i.e. arrays which are infinite along the y-direction, and semi-infinite along x, as shown in Fig. 1. The algorithm was based on the Shanks method [2] and was accurate for points close to the array plane. One of the authors has derived an asymptotic formula for the SAGF for observation points that are not too close to the edge of the array [3], [4]. As shown in [5], [6] and [7], the SAGF function is used as an excitation in the method of moments for the estimation of the effects of array truncation. Furthermore, the SAGF can be used to evaluate the field radiated by an array in presence of a scattering environment, as shown in [8].

In this Communication, to further accelerate the algorithm presented in [1], we use the Levin T accelerator [9] instead of the Shanks method. We show that it provides accurate results for points not too far (up to several wavelengths) from the array, but that a direct application of the Levin method (as well as the Shanks method in [1]) can result in large errors for some conditions of phasing and observation height. We show that these large errors are avoided when we apply the "flip" procedure, i.e., when the SAGF is evaluated by subtracting the GF of the complementary problem from the infinite-array GF. For larger distances from the array (several wavelengths), asymptotic formulas are given here for the scalar SAGF, instead of for the electric field as in [3]. Numerical results indicate the z-distance from the array plane where the asymptotic

Manuscript received August 11, 2005. This work was supported by the EU-funded project METAMORPHOSE (FP6/NMP3-CT-2004-500252).

C. Craeye is with the Université Catholique de Louvain, Laboratoire TELE, 1348 Louvain-la-Neuve, Belgium (e-mail: craeye@tele.ucl.ac.be).

F. Capolino is with the University of Siena, Department of Information Engineering, 53100 Siena, Italy (e-mail: capolino@dii.unisi.it).

Digital Object Identifier 10.1109/TAP.2006.869945

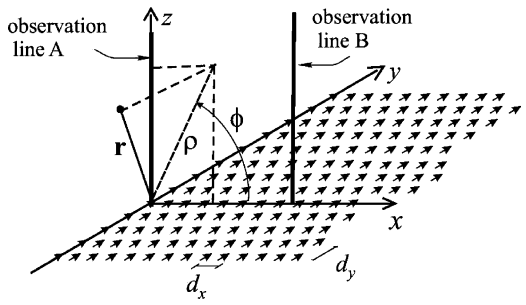

Fig. 1. Geometry of the semi-infinite array of parallel dipoles. The array is truncated in the x-direction and infinite along the y direction. The cylindrical coordinate system is used in the asymptotic result.

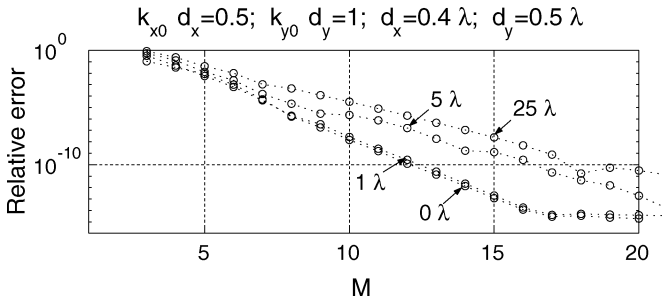

Fig. 2. Relative error of the Green's function for a semi-infinite array, as a function of the number of m terms, for an observation point located in the middle of the first unit cell. Obtained using the Levin T extrapolation procedure, for different heights of the observation point indicated next to the curves.

formula becomes more accurate than the Levin T formulation obtained with a given number of terms.

II. Statement of the Problem

The geometry of the array of phased dipole elements with impressed current, all oriented along the same direction, radiating in free space, is shown in Fig. 1. The array is infinite in the y direction and truncated in the x direction. Both cartesian and cylindrical reference coordinate systems, with cylindrical axis along the array edge, are introduced such that the array occupies the region $x > 0$, $z = 0$. The interelement spacings are d_x and d_y along the x and y directions, respectively. Bold face symbols define vector quantities. The dipole sources are located at $\mathbf{r}'_{mn} = (md_x, nd_y, 0)$, with $m = 0, 1, 2, \ldots$ and $n = 0, \pm 1, \pm 2, \ldots$. The SAGF for the vector magnetic potential produced by the parallel dipoles and evaluated at an arbitrary location $\mathbf{r} \equiv (x, y, z)$, is represented by the scalar potential

$$A(\mathbf{r}) = \sum_{m=0}^{\infty} \sum_{n=-\infty}^{\infty} \frac{e^{-jkR_{mn}}}{4\pi R_{mn}} e^{-jmk_{x0}d_x} e^{-jnk_{y0}d_y} \tag{1}$$

where k is the free space wave number, and R_{mn} is the distance between the observation point $\mathbf{r}$ and the mnth dipole. The terms k_{x0} and k_{y0} account for an assumed linear phase difference between adjacent elements in the x and y directions, respectively (a time dependence $\exp(j\omega t)$ is assumed and suppressed).

III. The Accelerated Line-by-Line Approach

As done in [1], the SAGF is conveniently expressed by summing the scalar potential contributions of all the infinite y-directed linear arrays, each one being represented by a spectral sum of cylindrical waves via the zeroth-order Hankel function of second kind

$$A(\mathbf{r}) = \sum_{q=-\infty}^{\infty} \frac{e^{-jk_{yq}y}}{4j\,d_y} \sum_{m=0}^{\infty} H_0^{(2)}(k_{\rho q}R_m) e^{-jmk_{x0}d_x}. \tag{2}$$

Here, $R_m = \sqrt{(x - md_x)^2 + z^2}$ corresponds to the distance to successive lines of dipoles, denoted by index m; $k_{yq} = k_{y0} + 2\pi q/d_y$ is the qth Floquet wavenumber along y, and

$$k_{\rho q} = \begin{cases} \sqrt{k^2 - k_{yq}^2}, & k^2 > k_{yq}^2 \\ -j\sqrt{k_{yq}^2 - k^2}, & k^2 < k_{yq}^2 \end{cases} \tag{3}$$

is the Floquet radial wavenumber of the qth cylindrical harmonic. Hereafter this method is called the "line-by-line" approach. For the radially evanescent q-harmonics (with imaginary $k_{\rho,q}$), the Hankel functions have an imaginary argument and the sums in (2) over both q (successive harmonics) and m (successive lines) are exponentially converging.

In this Communication, the m-series of propagating cylindrical waves (with real $k_{\rho,q}$) is further accelerated with the help of the Levin T transform, which already proved powerful for the acceleration of other periodic Green's functions as in [9]. In the following, we specialize the formula given in [9] to $n = 1$, which provides the highest degree of extrapolation. Denoting with $S_i = \sum_{m=0}^{i}(\cdot)$ the successive values of the m-sum in (2), the extrapolated value for the m-sum is

$$S^{ex} = \frac{\sum_{i=0}^{M}(-1)^i C_i^M \left(\frac{i+1}{M+1}\right)^{M-1} \frac{S_{i+1}}{S_{i+2} - S_{i+1}}}{\sum_{i=0}^{M}(-1)^i C_i^M \left(\frac{i+1}{M+1}\right)^{M-1} \frac{1}{S_{i+2} - S_{i+1}}} \tag{4}$$

where C_i^M is the binomial coefficient. Note that only the values from S_0 to S_{M+2} are required (i.e., the potential generated by only the first $M+3$ lines). The Levin T transform is more elaborated than the Shanks transformation, and it involves coefficients whose calculation may take a significant portion of the overall computation time. The latter, however, can be tabulated. In [9], the Levin T accelerator is applied to the doubly spectral-sum formulation of the GF for infinite-by-infinite arrays.

In Fig. 2 we illustrate the efficiency of the Levin accelerator by computing the SAGF for the same problem as in [1, Fig. 2]. The SAGF is thus computed for observation points $\mathbf{r} = (0.5d_x, 0.5d_y, z)$, with heights $z =$ 0,1,5 and 25 wavelengths λ. The relative error is evaluated against a more accurate reference SAGF still evaluated with (4), but with $M = 30$. From the results in Fig. 2 we infer that the convergence rate is exponential, which is much faster than when using the Shanks transform, that provides convergence of the order of $1/m^2$ [1]. In the on-plane case ($z = 0$), for instance, the first order Shanks transform would take about $m = 200$ propagating cylindrical waves to achieve a relative error equal to 10^{-8}, while here, the Levin T accelerator needs only $m = 10$ propagating cylindrical waves to achieve the same accuracy. As will be explained in the following, the convergence rate slightly decreases for observation points away from the array plane.

IV. Asymptotic Solution

We report here asymptotic closed forms for the *scalar* potential based on the results presented in [3], [4] for the electric field. Without loss of generality, due to symmetry, we restrict our analysis to the upper half-space $z > 0$. The radiated potential is expressed as

$$A(\mathbf{r}) = \sum_{p,q=-\infty}^{\infty} A_{pq}^{\mathrm{FW}}(\mathbf{r}) U\left(\phi_{pq}^{SB} - \phi\right) + \sum_{q=-\infty}^{\infty} A_q^d(\mathbf{r}) \tag{5}$$

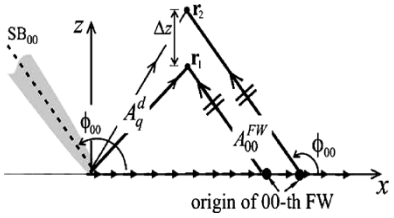

Fig. 3. Transverse-to-y domain for the semi-infinite array. The 00th FW exists on the right side of its shadow boundary (SB), the abrupt FW discontinuity is repaired by the 0th diffracted field. Higher order pq FWs and q diffracted fields are in general evanescent, along z and ρ, respectively. Distinct points $\mathbf{r}_1$ and $\mathbf{r}_2$ are reached by two parallel rays that are the 00th FW with shifted origin.

which contains an infinite series of (pq)-indexed FW contributions $A_{pq}^{\mathrm{FW}}(\mathbf{r})$, and q-indexed diffracted fields $A_q^d(\mathbf{r})$ arising from the edge of the array. The pqth FW in (5) is given by

$$A_{pq}^{\mathrm{FW}}(\mathbf{r}) = \frac{e^{-j(k_{xp}x+k_{yq}y+k_{zpq}z)}}{2jd_xd_yk_{zpq}} \tag{6}$$

and $U(\alpha) = 1$ or 0 for $\alpha > 0$ or $\alpha < 0$, respectively. The spectral wavenumbers $k_{xp} = k_{x0} + 2\pi p/d_x$, $k_{yq} = k_{y0} + 2\pi q/d_y$, represent the FW propagation wavenumbers along x and y, respectively. Furthermore, $k_{zpq} = (k^2 - k_{xp}^2 - k_{yq}^2)^{1/2}$ characterizes propagating FWs for $k^2 > k_{xp}^2 + k_{yq}^2$ and FWs evanescent along z for $k^2 < k_{xp}^2 + k_{yq}^2$, since in this case $k_{zpq} = -j|k_{zpq}|$. It is worth noting that the FW representation in (6) is the same as that for the infinite array, except for the Heaviside unit step function U in (5) that confines the domain of existence of the pqth FWs to the region $\phi < \phi_{pq}^{SB}$ (see Fig. 3 and [3]). The angle ϕ_{pq}^{SB} denotes the shadow boundary (SB) of the pqth FW and, for propagating FWs, is given by [3, eq.(24)]$\phi_{pq}^{SB} = \phi_{pq} = \cos^{-1}(k_{xp}/k_{\rho q})$, with $k_{\rho q}$ given in (3), which also specifies the direction of the azimuthal component (in the (x,z) plane) of the propagating pqth FW wavenumber.

The asymptotic evaluation of the qth diffracted field in (5) is carried out in [3, Sec.III-B] for the electric field, and adapted here to the scalar potential

$$A_q^d(\mathbf{r}) \sim \frac{e^{-j(k_{\rho q}\rho + k_{yq}y)}}{2d_y\sqrt{2\pi j k_{\rho q}\rho}} \left\{ B_q + \sum_{p=-P}^{P} \left(W_{pq-}\left[F\left(\delta_{pq-}^2\right) - 1\right] + \epsilon_p W_{pq+}\left[F\left(\delta_{pq+}^2\right) - 1\right]\right)\right\} \tag{7}$$

in which $\rho = (x^2+z^2)^{1/2}$, $B_q = [1 - e^{jd_x[k_{\rho q}\cos\phi - k_{x0}]}]^{-1}$, $W_{pq\pm} = -[2jk_{zpq}d_x \sin((\phi_{pq} \pm \phi)/2)]^{-1}$, $\epsilon_p = \mathrm{sgn}(k_{xp})$ and F is the transition function of the uniform theory of diffraction (UTD) [10], (see also [3]) whose arguments are $\delta_{pq\pm} = \sqrt{2k_{\rho q}\rho}\sin[(\phi \pm \phi_{pq})/2]$. In (6) and (7), for an accurate approximation a few wavelengths away from the array, the p, q-sums extend to all possible propagating FWs (see [3, eq.(25)] due to the exponential attenuation of the evanescent Floquet and diffracted waves along z and ρ, respectively. Thus, in practice, only a few terms, those propagating, have to be retained in (5) to provide excellent approximations of the radiated field [4, Sec.II-B].

V. Performance of the Line-by-Line and Asymptotic Approaches

In this section we show the relative error of the scalar potential radiated by the semi-infinite array of dipoles, evaluated with the Levin T accelerator (Section III) using only the potential radiated by the first 10 lines [$M = 7$ in (4)] and the asymptotic formula in Section IV. When evaluating the SAGF with the Levin T accelerator, it may be convenient to use the decomposition

$$A = A_{ele}(N) + A_L(N) \tag{8}$$

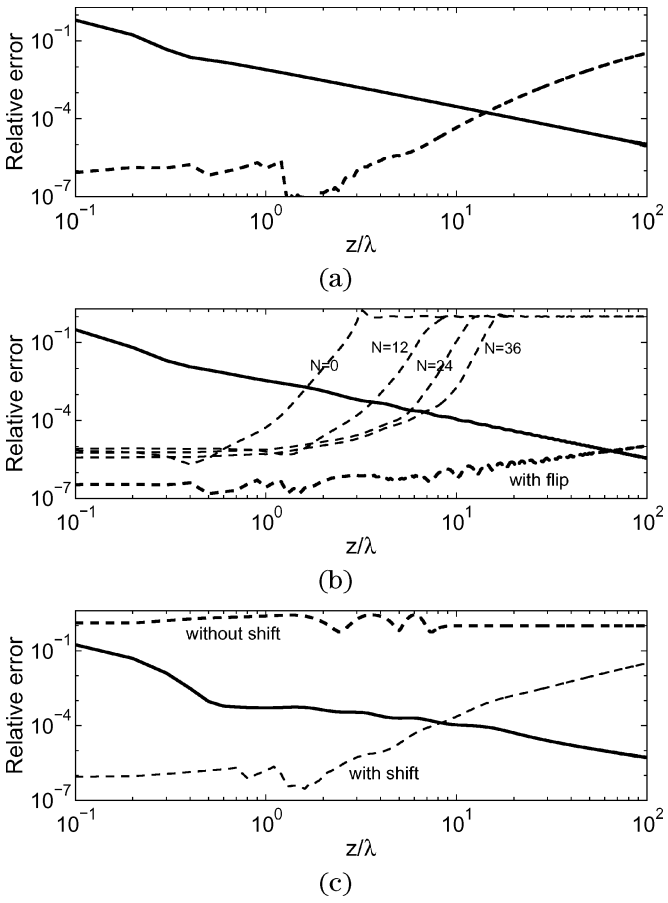

Fig. 4. Relative error of the SAGF for observation points along lines A and B of Fig. 1. $k_{y0} = 0$. Tick solid: asymptotic approach. Thick dashed: line-by-line with $M = 7$. (a) Line A, $k_{x0} = 0$. (b) line A, $k_{x0} = -0.8$ k. Thin dashed: with shift, for different N's in (8). (c) Line B, $k_{x0} = 0$. Without and with $(N = 10)$ shift.

where $A_{ele}(N)$ is the potential radiated by the first N linear arrays, and $A_L(N)$ is the potential radiated by the remaining semi-infinite array, evaluated with the help of the Levin T accelerator (4). The reason for doing this is to limit the number M in (4) that otherwise needs to be too large for certain array phasings. Indeed, round-off errors arise in (4) because the numerator and denominator become excessively large for large M. The relative error in Fig. 4 is evaluated against a reference -and significantly slower- solution decomposed as in (8) with $N = 20$ and by using a large value $M = 25$ in A_L.

The array considered as an example has element spacings $d_x = d_y = 0.4\lambda$. The potential is evaluated along the two vertical lines, A and B, shown in Fig. 1, located at $x = 0$ and $x = 5\lambda$, respectively, and ranging from $z = 0.1\lambda$ to $z = 100\lambda$.

In all cases in Fig. 4, the line-by-line approach in (4) (dashed curves) looses accuracy when moving away from the array plane, while the accuracy of the asymptotic approach (5) (continuous curve) improves. At a certain height z, the two methods have comparable accuracy.

The first result in Fig. 4(a) pertains to a SAGF evaluated along line A and radiated by an array with phasings $k_{x0} = 0$ and $k_{y0} = 0$. Note that the line-by-line approach starts to loose accuracy at $z \approx 3\lambda$. In order to understand this phenomenon, it is convenient to consider the phase Φ_m of the potential A_m radiated by he mth linear array. For the $q = 0$ harmonic, the phase Φ_m is well approximated by the mth contribution in (2)

$$\Phi_m \approx k_{x0}md_x + k_{\rho 0}\left[z^2 + \left(x - m^2d_x^2\right)\right]^{\frac{1}{2}}. \tag{9}$$

For the particular phasing considered here, and for observation points away from the array, the contributions from the first linear arrays (small m) are similar in terms of amplitude $|A_m|$ and phase Φ_m. A clear amplitude and phase trend of the potential A_m from a mth linear array is established only for larger values of m. It seems that, in order to provide a very good convergence, the Levin T accelerator (4) needs a clear trend of A_m for values of m close to M, which is the number of linear arrays used in (4) to extrapolate the total potential. In the following, we analyze the phase trend Φ_m of the elements with $m \approx M$.

For the case in Fig. 4(a), when z is larger than 3λ, the phase Φ_m for $m \approx M = 7$ departs from being linear and it approaches the quadratic behavior in m with a vanishing slope versus m. This phenomenon is confirmed by another numerical experiment, in Fig. 4(b), that pertains to the same array but with phasing $k_{x0} = -0.8$ k and observation points along the line A. The line-by-line approach converges for small z and becomes very inaccurate $(\text{error} = 1)$ for $z_0 \approx 3\lambda$, which, according to (9), coincides with the region where the phase Φ_m has a vanishing variation versus m ($\partial\Phi_m/\partial m = 0$ where m is now extended to the real domain [11]). In [3], [4], and [11] it was demonstrated that the point in Fig. 3 where the 00th Floquet wave originates from the array plane coincides with that point where the phase variation Φ_m vanishes, which depends on the location of the observation point. In other terms, the line-by-line approach loses accuracy when the Levin T accelerator is truncated before or in the region where the Floquet wave originates, because, there, the Φ_m phase trend is not clearly established.

The consistency of this hypothesis is further confirmed by the analysis of what happens when we extend the truncation area of the Levin extrapolator. However, instead of using large values of M in (4), we use the decomposition (8): M is kept equal to 7, while the contributions from N linear arrays are successively added before performing the Levin extrapolation. In this way, the truncation region of the Levin extrapolator is around the $(N+M)$th linear array. Fig. 4(b) shows that the line-by-line approach, now decomposed as in (8) with $N = 12$, becomes very inaccurate for $z_2 \approx 8.8\lambda$, and decompositions with $N = 24$ and 36 become very inaccurate for $z_3 \approx 12.6\lambda$ and $z_4 \approx 16.5\lambda$, respectively. Therefore, the same accuracy is maintained if, to height increments of $\Delta z \approx z_4 - z_3 \approx z_3 - z_2 \approx 3.8\lambda$, correspond increments of $N = 12$ linear arrays in the decomposition (8). Note that the ratio $\Delta z/(12d_x) \approx 0.79$ is very close to $\tan(\pi - \phi_{00}) = 0.75$, where $\phi_{00} = \cos^{-1}(k_{x0}) \approx 143^\circ$ is the direction of propagation of the $(p,q) = (0,0)$ Floquet wave (see Fig. 3).

A simple solution to this problem is obtained by avoiding the evaluation of fields from semi-infinite arrays containing a stationary-phase point. The curve labeled "with flip" in Fig. 4(b) represents the potential evaluated as $A = A^{\text{inf}} - A^{\text{compl}}$, where A^{inf} is the potential radiated by an infinite planar array and A^{compl} is the potential from the complementary array that occupies the region $x < 0$ (that is why we call it *with flip*). The line-by-line approach is applied to A^{compl} whose Φ_m is now very regular because there are no Floquet waves arising from the complementary array for this kind of phasing [3], [4]. The accuracy of the line-by-line approach with "flip" is very satisfactory.

In Fig. 4(c) the array phasing is $k_{x0} = 0$, and the observation point is now along the line B of Fig. 1. The line-by-line approach with $N = 0$ and $M = 7$ is not accurate because the observation point is illuminated by the 00th Floquet wave that originates from a point that does not lay in the region $m = 0, \ldots, M$ and therefore cannot be properly accounted for by the Levin T accelerator. If the decomposition (8) with $N = 10$ is applied, the origin of the Floquet wave is correctly accounted for when the observer is not too far from the array, and the line-by-line approach provides a very accurate result.

In all cases considered, the accuracy of the SAGF evaluated with the asymptotic formula (5) improves away from the array and the error in dB decreases as $30\log z$, which corresponds to an error decay of $1/z^{3/2}$. Indeed, the asymptotic evaluation in (5) considers only the first order diffracted field $A_q^d(\mathbf{r})$ which decays as $1/\rho^{1/2}$, with $\rho = (x^2 + z^2)^{1/2}$, and the asymptotic error is the next missing asymptotic term, with decay $1/\rho^{3/2}$ [3], [4].

VI. Conclusion

We have shown that the line-by-line approach presented in [1] for the semi-infinite array Green's function (SAGF) and here combined with the use of the Levin T accelerator leads to exponential convergence rates. The convergence rate decreases away from the array plane, where asymptotic results, as those formulated in [3], [4], provide instead faster results for a given accuracy, and therefore should be preferably used for these observation aspects. The exponential convergence makes the line-by-line approach combined with the Levin T accelerator faster than the Shanks method for an accurate evaluation of the SAGF not too far from the array plane. The convergence of the Levin T accelerator for the semi-infinite array has been discussed and explained by resorting to the wave dynamics associated to the problem. In particular, we have shown that the origin of the radiated Floquet waves must be included in the region that is used by the Levin T accelerator to extrapolate the total potential radiated by the semi-infinite array and the decomposition (8) is applied for this purpose. When this decomposition is not sufficient, the "flip" operation (the total potential evaluated as the one from the infinite array minus that of the complementary one) is useful to automatically regularize the first M partial sums in (4).

References

[1] C. Craeye, A. B. Smolders, A. G. Tijhuis, and D. H. Schaubert, "An efficient computation scheme for the free-space Green's function of a two-dimensional semi-infinite phased array," *IEEE Trans. Antennas Propag.*, vol. 51, no. 4, pp. 766–771, Apr. 2003.

[2] D. Shanks, "Nonlinear transformation of divergent and slowly convergent sequences," *J. Math. Phys.*, vol. 34, pp. 1–42, 1955.

[3] F. Capolino, M. Albani, S. Maci, and L. B. Felsen, "Frequency-domain Green's function for a planar periodic semi-infinite phased array—part I: truncated Floquet wave formulation," *IEEE Trans. Antennas Propag.*, vol. 48, no. 1, pp. 67–74, Jan. 2000.

[4] ——, "Frequency domain Green's function for a planar periodic semi-infinite dipole array. Part II: phenomenology of diffracted waves," *IEEE Trans. Antennas Propag.*, vol. 48, no. 1, pp. 75–85, Jan. 2000.

[5] A. Neto, S. Maci, G. Vecchi, and M. Sabbadini, "Truncated Floquet wave diffraction method for the full wave analysis of large phased arrays—Part II: Generalization to the 3-D case," *IEEE Trans. Antennas Propag.*, vol. 48, no. 4, pp. 600–611, Apr. 2000.

[6] C. Craeye, A. G. Tijhuis, and D. H. Schaubert, "An efficient MoM formulation for finite-by-infinite arrays of two-dimensional antennas arranged into a three-dimensional structure," *IEEE Trans. Antennas Propag.*, vol. 52, no. 1, pp. 271–282, Jan. 2004.

[7] C. Craeye, "Fast computation and etrapolation of the effects of array truncation in broadband anntenna arrays," in *Proc. IEEE AP-S Symp.*, Columbus, OH, Jun. 2003.

[8] F. Capolino, S. Maci, M. Sabbadini, and L. B. Felsen, "Large phased arrays on complex platforms," presented at the *Int. Conf. Electromagnetics and Advanced Appl. ICEAA* , Torino, Italy, Sep. 2001.

[9] S. Singh and R. Singh, "On the use of Levin's T-transform in accelerating the summation of series representing the free-space periodic Green's function," *IEEE Trans. Microwave Theory Tech.*, vol. 41, pp. 884–886, May 1993.

[10] R. G. Kouyoumjian and P. H. Pathak, "A uniform geometrical theory of diffraction for an edge in a perfectly conducting surface," *Proc. IEEE*, vol. 62, pp. 1448–1461, Nov. 1974.

[11] L. B. Felsen and L. Carin, "Frequency and time domain Bragg-modulated acoustic for truncated periodic array," *J. Acoust. Soc. Amer.*, vol. 95, no. 2, pp. 638–649, Feb. 1994.